Bimetallic catalysts as dissipative structures: stationary concentration patterns in the $O_2 + H_2$ reaction on a composite Rh(110)/Pt surface

E. Schütz [a], F. Esch [b], S. Günther [b], A. Schaak [a], M. Marsi [b], M. Kiskinova [b] and R. Imbihl [a]

[a] *Institut für Physikalische Chemie und Elektrochemie, Universität Hannover, Callinstrasse 3–3a, D-30167 Hannover, Germany*
[b] *Sincrotrone Trieste, Area Science Park-Basovizza, I-34012 Trieste, Italy*

Received 15 July 1999; accepted 21 September 1999

The $O_2 + H_2$ reaction has been studied under low pressure conditions (10^{-5} mbar) employing a microstructured Rh(110)/Pt surface as catalyst. Photoemission electron microscopy (PEEM) and scanning photoelectron microscopy (SPEM) were used as spatially resolving *in situ* methods. Under reaction conditions stationary concentration patterns (Turing-like structures) of the adsorbates develop inside the Pt domains which are associated with a compositional change of the metallic substrate.

Keywords: bimetallic catalysts, platinum, rhodium, $O_2 + H_2$ reaction, pattern formation, scanning photoelectron microscopy (SPEM), photoelectron emission microscopy (PEEM), Turing structure

Catalytic reactions are typically thought of as taking place on a rigid surface with a fixed composition and structure. Such a static picture, however, is misleading since dynamic instabilities may not only lead to the formation of chemical wave patterns but they may even alter structure and composition of the catalyst itself [1–3]. In this paper we report on the observation of stationary concentration patterns in a simple surface reaction, namely the $H_2 + O_2$ reaction. We have studied this reaction on a composite catalyst consisting of microstructured Pt domains on a Rh(110) surface. Inside the Pt domains stationary concentration patterns of the adsorbates evolve which are associated with a compositional change of the metallic Pt/Rh substrate. These stationary patterns provide a striking example for the importance of dynamic effects in catalysis because, in our case, the metal catalyst itself represents a dissipative structure.

To construct a microstructured model catalyst we employ a negative photoresist process in which we deposit a thin Pt layer (300 Å thick) onto a Rh(110) single crystal surface [4,5]. In this way Pt domains of varying size and geometry are created surrounded by Rh(110). We study the reaction $(1/2)O_2 + H_2 \rightarrow H_2O$ which is catalyzed by both metals, Pt and Rh [6,7]. Hydrogen and oxygen each adsorb dissociatively on Pt and Rh and the atomic adsorbates react to the product H_2O which rapidly desorbs. In the parameter range investigated here the reaction on each metal exhibits simple mono- or bistable behaviour.

We conduct our measurements under isothermal conditions at low pressure ($p < 10^{-4}$ mbar) operating our ultrahigh vacuum chamber as a continuous flow reactor. For spatially resolved *in situ* measurements two methods are applied, first photoemission electron microscopy (PEEM) [8], which images the local work function but yields no direct information about the chemical identity of the adsorbed species and the chemical state and the composition of the catalyst surface. The missing chemical information is provided by scanning photoelectron microscopy (SPEM) [9]. In SPEM photons (300–900 eV) from a synchrotron source (ELETTRA) are focused into a 0.15 μm spot on the sample. While the sample is scanned photoelectrons are collected with a hemispherical energy analyser tuned to the energy of a specific core level. In this way 2D-maps of the elemental distribution are generated.

The PEEM images in figure 1 show various stationary concentration patterns we observe inside the Pt domains under reaction conditions. We attribute the bright spots, which develop inside the Pt domains several minutes after the adjustment of pO_2 and pH_2, to the presence of an oxygen species with negative dipole moment [12,13]. Such a species lowers the work function thus increasing the brightness in PEEM in contrast to the usual chemisorbed oxygen which appears as dark area in PEEM. A subsurface oxygen species will presumably have such a negative dipole moment but, alternatively, also other species like an OH intermediate should not be excluded [10,11]. Remarkably, this oxygen species which is characterized by a reduced work function in PEEM ony forms under reaction conditions but not in simple adsorption experiments.

The formation of the stationary patterns is completely reversible and, as demonstrated by figure 1 (a)–(d), size and geometry dependent. The different types of patterns reproduced in figure 1 (a)–(d) were obtained by varying the control parameters pH_2 and temperature, while pO_2 was kept fixed at $pO_2 = 2 \times 10^{-6}$ mbar. Under certain conditions

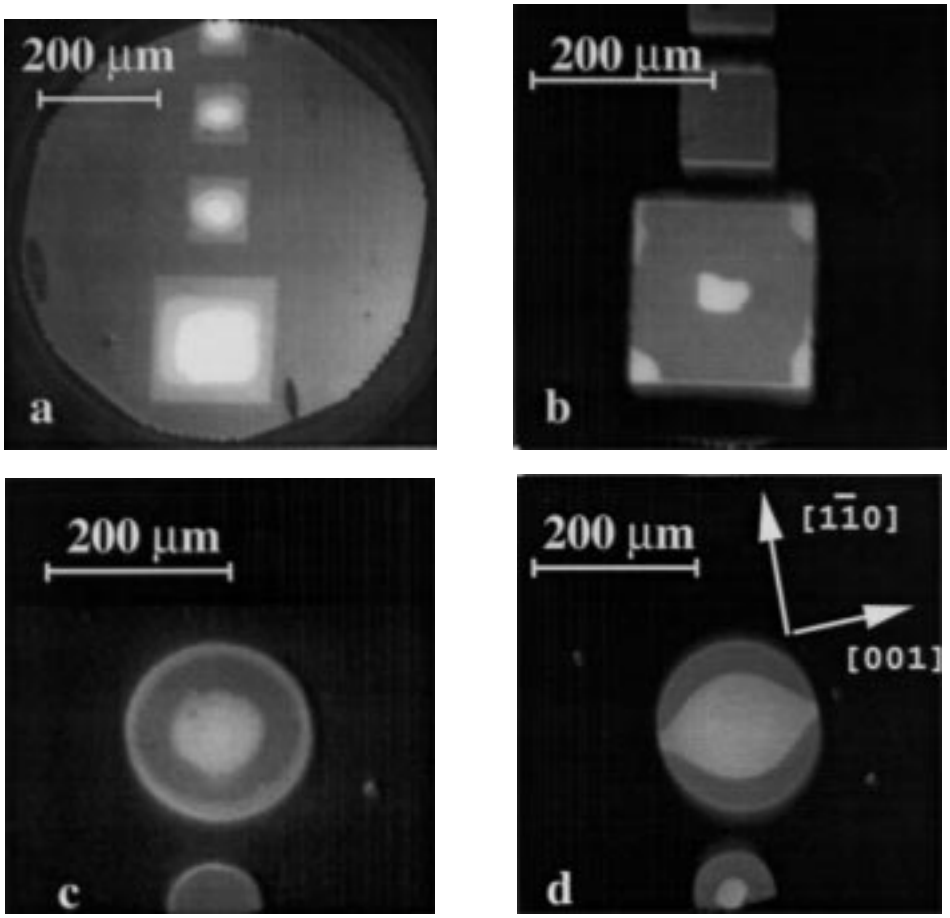

Figure 1. PEEM images showing the formation of stationary concentration patterns during the $O_2 + H_2$ reaction on a microstructured Rh(110)/Pt surface. The squares and circles represent Pt domains surrounded by the Rh(110) surface. The crystallographic directions of the Rh(110) surface are indicated for all PEEM images in (d). All images are shown with the same grey scale. (a) Stationary patterns inside Pt squares. Experimental conditions: $p\mathrm{O}_2 = 2.0 \times 10^{-6}$ mbar, $p\mathrm{H}_2 = 1.7 \times 10^{-6}$ mbar, $T = 551$ K. (b) Centered structure in a Pt square. Experimental conditions: $p\mathrm{O}_2 = 2.0 \times 10^{-6}$ mbar, $p\mathrm{H}_2 = 1.7 \times 10^{-6}$ mbar, $T = 478$ K. (c) Stationary pattern with two bright zones inside a large Pt circle. Experimental conditions: $p\mathrm{O}_2 = 2.0 \times 10^{-6}$ mbar, $p\mathrm{H}_2 = 1.2 \times 10^{-6}$ mbar, $T = 526$ K. (d) Symmetry breaking of patterns inside Pt circles caused by anisotropic diffusion on the surrounding Rh(110) surface. Experimental conditions: $p\mathrm{O}_2 = 2.0 \times 10^{-6}$ mbar, $p\mathrm{H}_2 = 1.4 \times 10^{-6}$ mbar, $T = 476$ K. The temperature varied slightly in this experiment.

centered structures develop as shown by figure 1(b). Inside large circles several brightness zones form as depicted in figure 1(c). The diffusion anisotropy of the surrounding Rh(110) surface, which has an atomic surface structure consisting of troughs oriented along [110], can lead to symmetry breaking inside the circular domains, as demonstrated by figure 1(d) [12].

We can describe our composite reaction system Rh(110)/Pt/$O_2 + H_2$ as two bistable media coupled by a fast diffusing species, atomic hydrogen [13]. Both metals can either be in an unreactive high oxygen coverage state or in a reactive low oxygen coverage state [6,7]. It depends on the relative reactivity of the two metal surfaces whether the Rh/Pt interface acts as a source or a drain for diffusing hydrogen inside the Pt domain. The strong diffusional coupling of Pt and Rh(110) becomes particularly evident in figure 1(d), where the pattern inside the Pt domain reflects the anisotropy of the surrounding Rh(110) surface. Diffusion on this surface is fast along the [110]-oriented troughs and slow perpendicular to them.

Figure 2 displays the existence ranges for the stationary (Turing-like) patterns which have been mapped out in $p\mathrm{H}_2$–T parameter space at a fixed oxygen partial pressure, $p\mathrm{O}_2 = 2 \times 10^{-6}$ mbar. On the Rh(110) surface which surrounds the Pt domains the reaction is bistable and the bold line in the diagram divides the parameter space into two ranges: left to the equistability line the surface is in a stable oxygen-covered state and to the right an almost oxygen-free Rh(110) surface is the stable state of the system. The location of this equistability line was determined by decreasing $p\mathrm{H}_2$ starting from a high value down to the point where reaction fronts start to nucleate on the Rh(110) surface. These fronts initiate a transition from the low oxygen coverage to the high oxygen coverage state. As was shown in an earlier study, the $p\mathrm{H}_2$ values at which this transition occurs are located very close to the actual equistability line in the bistable system Rh(110)/$O_2 + H_2$ [6].

Adjacent to the equistability line in figure 2 we find two parameter ranges, T_1 and T_2, inside which we observe stationary patterns on the Pt domains. In T_1 located right of the

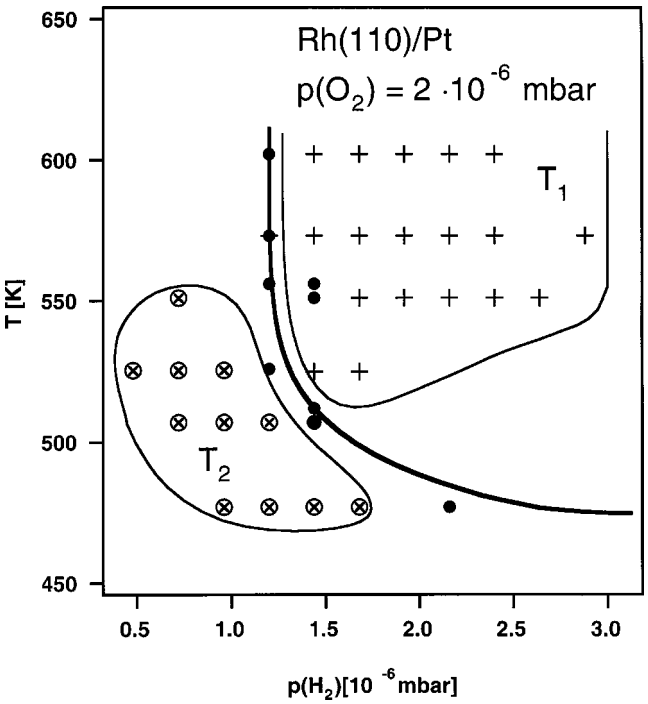

Figure 2. Existence diagram for the formation of stationary concentration patterns in the system Rh(110)/Pt/$O_2 + H_2$. T_1 and T_2 denote the two existence ranges for the formation of Turing-like structures on Pt domains. The bold line represents approximately the equistability line for the bistable system Rh(110)/$O_2 + H_2$, i.e., left of this line the Rh(110) surface surrounding the Pt domains is in a stable oxygen-covered state, to the right a nearly oxygen-free Rh(110) surface is seen.

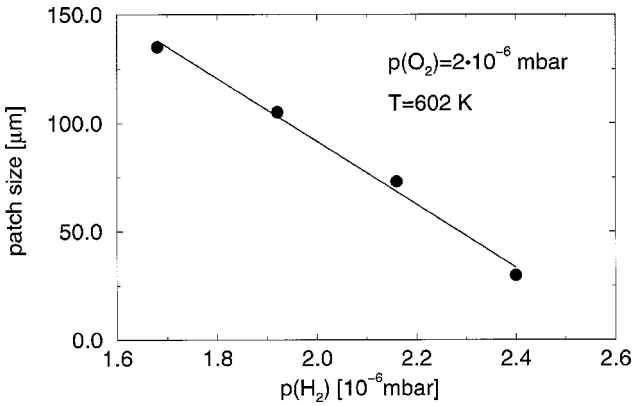

Figure 3. Dependence of the size of the low work function areas (bright patches in PEEM) in the Turing-like structures on pH_2. The diameter of a bright patch in the center of a 200×200 μm^2 Pt domain was measured for varying pH_2 inside the existence range T_1.

equistability line we expect that the surrounding Rh(110) surface acts as a source of hydrogen for the Pt domains because on the nearly oxygen-free surface the adsorption of hydrogen is not inhibited; in T_2 the Rh(110) surface should serve as a sink for hydrogen because a large oxygen coverage inhibits H_2 adsorption. In agreement with this simple picture we see that in the patterns belonging to T_1 (figure 1(a)) no oxygen (bright areas) is found in the edge regions presumably because the oxygen is reacted off by hydrogen diffusing from the nearly oxygen-free Rh(110) surface into the Pt domains. Consistent with this interpretation one finds in the patterns of figure 1 (b)–(d) which all belong to T_2 high oxygen concentrations also in the edge regions of the Pt domains. In figure 1 (b)–(d) we note a bright edge zone, hardly visible in figure 1 (b) and (d), which is not present in figure 1(a). When we vary pH_2 the size of the bright patches changes until they finally disappear at the boundaries of their existence range. Figure 3 displays this dependence of the patch size on pH_2 for a bright patch located inside a 200×200 μm^2 Pt domain. Outside the existence range T_1 but close to the high pH_2 boundary one also observes non-stationary structures which are, however, transient. Figure 4 displays a rather peculiar structure which has the shape of a dogbone. This "dogbone" slowly rotates while it dissolves.

In order to investigate the chemistry of the system we conducted spatially resolved chemical mapping with SPEM at ELETTRA. Figure 5 displays 2D maps of the elemental distribution of oxygen, platinum and rhodium under reaction conditions under which a stationary pattern similar to figure 1(a) develops. The maps taken from a 90×90 μm^2 Pt square demonstrate that the central area not only contains

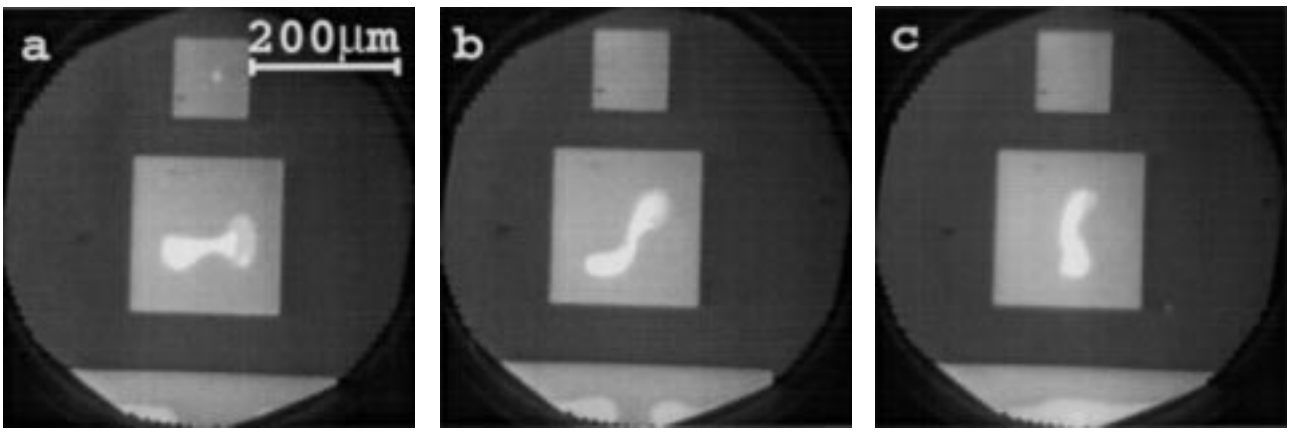

Figure 4. PEEM images showing instationary concentration patterns which appear as transients close to the boundary of T_1. The structure slowly rotates with a rotational period of ca. 30 min. Experimental conditions: $T = 598$ K, $pO_2 = 2.0 \times 10^{-6}$ mbar, $pH_2 = 4.32 \times 10^{-6}$ mbar. (a) $t = 0$, (b) 180 and (c) 360 s.

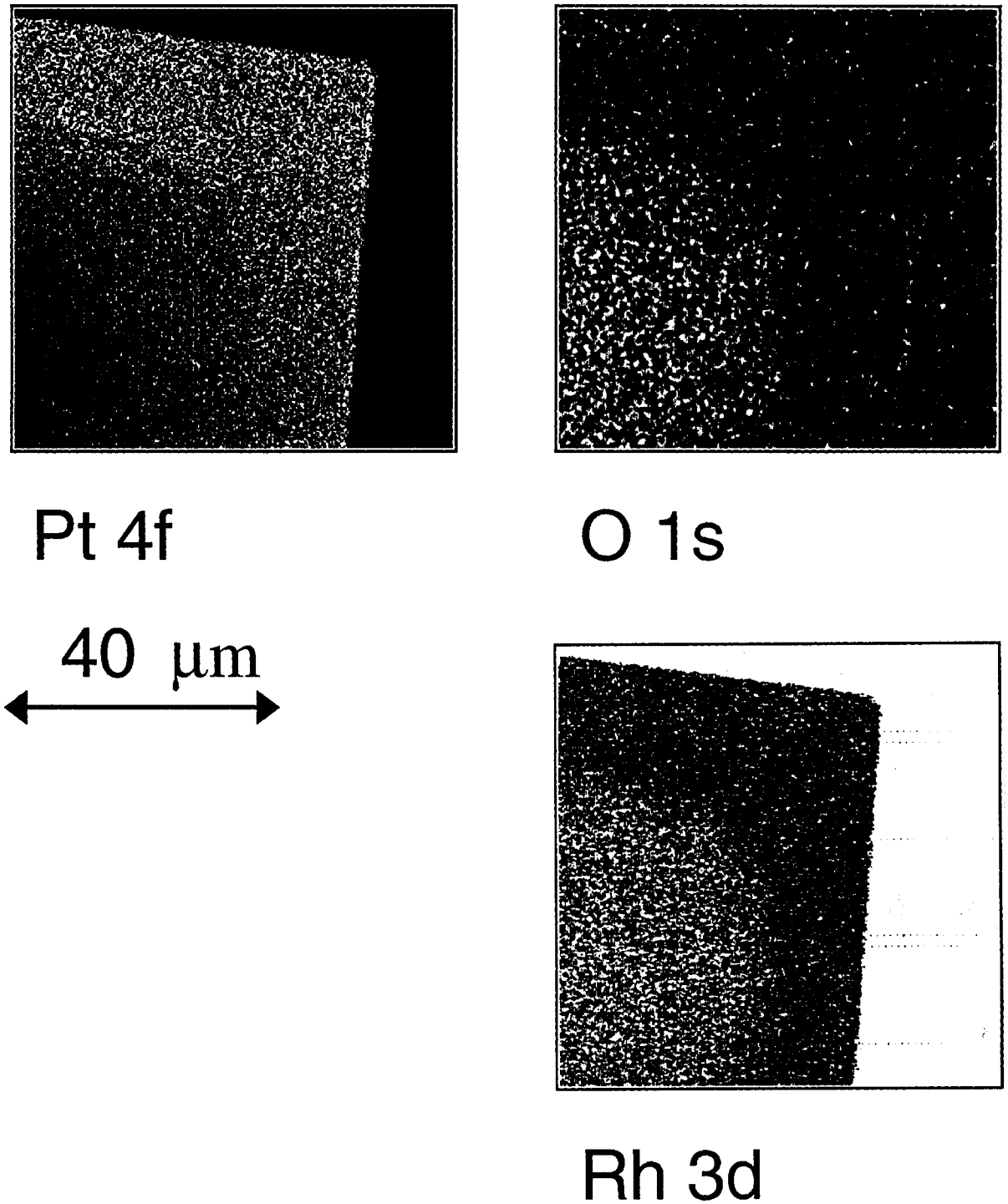

Figure 5. 2D maps recorded *in situ* with SPEM showing the elemental distribution in a stationary concentration pattern of the type depicted in figure 1(a). The images are taken from a 90×90 μm^2 Pt domain. Experimental conditions: $T = 600$ K, $pO_2 = 2 \times 10^{-7}$ mbar, $pH_2 = 1.7 \times 10^{-7}$ mbar. Photon energy = 620 eV. The intensities of the O 1s, Rh 3d and Pt 4f photoemission peaks have been mapped out. The maximum oxygen concentration, θ_O, is roughly 0.5, the Rh coverage on Pt varies between $\theta_{Rh} = 0.04$ and 0.29.

oxygen but that also, rather unexpectedly, Rh is present. The Rh apparently must have segregated from the 300 Å thick Pt film which contains some Rh due to vertical intermixing with the Rh(110) surface underneath. The enrichment of Rh on the Pt surface is reversible and bound to the stationary patterns. The reversibility of the Rh segregation is demonstrated in figure 6. The plots show the local Rh concentration evaluated from the Rh 3d peak of local photoelectron spectra taken inside a Pt domain. Figure 6(a) shows that the Rh slowly segregates to the surface in ∼30–40 min when we adjust reaction conditions under which a bright spots form. When the pattern forming parameter range is left, a Pt surface with the low Rh concentration initially present is established again within ca. 10 min as

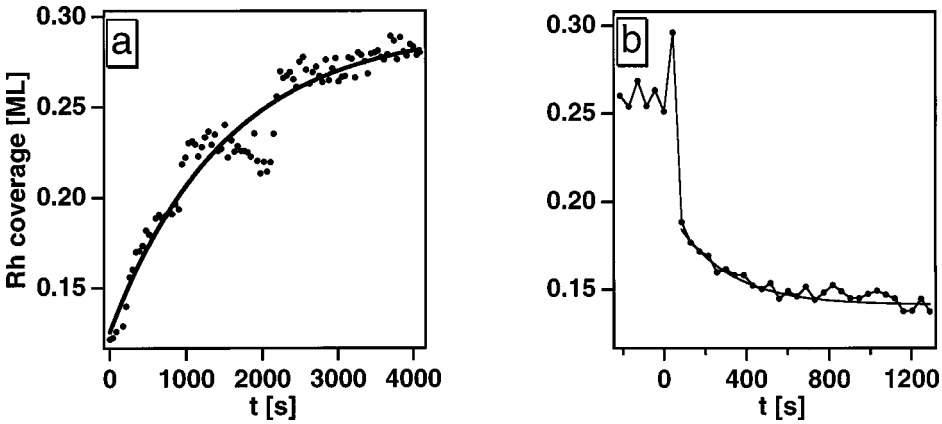

Figure 6. Reversible segregation of Rh in a Pt domain for varying reaction conditions, i.e., conditions which correspond to (a) development of a Turing-like structure and (b) reappearance of the spatially uniform state inside the Pt domain. The Rh concentration was determined in the center of a 90×90 μm^2 Pt domain. Experimental conditions: $T = 600$ K, $pO_2 = 2 \times 10^{-7}$ mbar, $pH_2 = 1.7 \times 10^{-7}$ mbar. (a) Formation of a bright spot in PEEM initiated at $t = 0$ by a decrease of pH_2 from 4.8×10^{-7} to 1.7×10^{-7} mbar. (b) Reappearance of the uniform state inside the Pt domain initiated by a pH_2 increase from 1.7×10^{-7} to 4.8×10^{-7} mbar at $t = 0$.

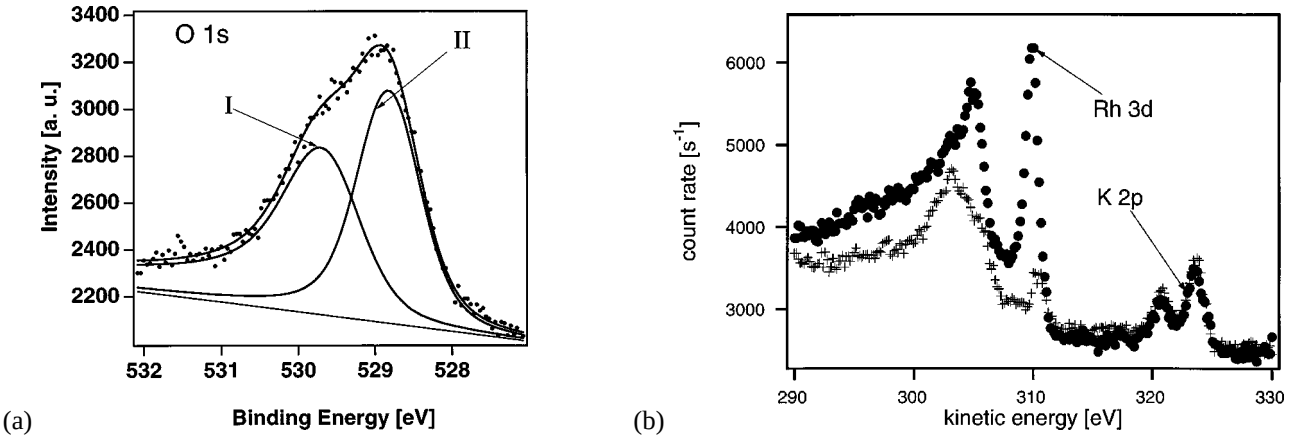

Figure 7. Local photoelectron spectra (0.15 μm spot size) taken inside the 90×90 μm^2 Pt domain showing the presence of different oxygen species and of potassium in the stationary patterns. Experimental conditions: $T = 600$ K, $pO_2 = 2 \times 10^{-7}$ mbar, pH_2 varying. (a) O 1s spectrum demonstrating the existence of at least two distinct oxygen species under the conditions of stationary (Turing-like) structures. The spectrum was taken at a position where in PEEM a bright spot is observed. A high concentration of species (II) was reached by a stepwise rise of pH_2 from 0 to 4.8×10^{-7} mbar; the spectrum was taken at $t = 8$ min. A decomposition of the experimental spectrum into two peaks with BEs of 529.7 eV (I) and 528.8 eV (II) is indicated. Species I is also observed in pure O_2 and apparently represents chemisorbed oxygen. (b) Photoelectron spectra showing the energy region with the Rh Auger, Rh 3d and K 2p peaks. The spectra were taken at two locations: (i) close to the Pt/Rh boundary (+) and (ii) in the center of the Pt domain (•). Experimental conditions: $pH_2 = 1.7 \times 10^{-7}$ mbar.

demonstrated by figure 6(b). The slow time scale can be attributed to the vertical diffusion of Rh in the Pt layer. The Rh surface concentration in these experiments varies between $\theta_{Rh} = 0.29$ and 0.04.[1]

An O 1s photoelectron spectrum taken inside one of the bright spots is reproduced in figure 7(a). The O 1s peak is clearly composed of at least two components. Species I with a BE of 529.7 eV can be assigned to chemisorbed oxygen and the BE of the second component of 528.8 eV would be consistent with an oxidic species [14]. Remarkably, this second species only forms under reaction conditions and we can therefore tentatively associate this component with the oxygen species responsible for the bright spot formation. The rhodium inside the oxygen patch, i.e., inside the bright areas visible in PEEM, exhibits a shift of 0.64 eV of Rh 3d towards higher binding energy with respect to the clean Rh(110) surface. The magnitude of this shift exceeds by far the shift we obtain for chemisorbed oxygen on Rh(110) of 0.16 eV. This indicates that some kind of mixed Pt/Rh oxide has been formed.

The photoelectron spectra also reveal that a significant amount of potassium is present on the surface originating probably from the lithographic process over which the microstructures were produced. The potassium is only found on Pt but not on the Rh surface. Figure 7(b) displays two photoelectron spectra taken at the edge region and at the center of the Pt domain. Both spectra show the same

[1] The Rh concentrations were calculated assuming that all of the Rh is located in the topmost metal layer and with one monolayer representing the number of Rh atoms of a Rh(110) surface.

amount of potassium. In spite of the missing correlation of the K concentration with the bright spots the comparison with data from the literature gives some indication that potassium might actually be involved in the formation of the bright spots. Photoelectron spectra taken after O_2 adsorption from a Pt(111) surface predosed with potassium show an O 1s BE in the range 528.9–529.5 eV, whereas regular chemisorbed oxygen on Pt(111) exhibits an O 1s BE of 530.2 eV [14,15].

The existence of stationary concentration patterns in a chemical reaction system has been predicted more than 40 years ago in a pioneering paper by Turing [16]. In this paper Turing proposed that stationary concentration patterns may develop in a reaction–diffusion (RD) system if the spatially homogeneous state is unstable with respect to a perturbation by diffusion. Although these so-called Turing patterns (TP) played a tremendous role as model systems for the development of biological structures [17], it took nearly 40 years until these patterns could finally be experimentally realised in chemical systems [18,19]. Turing patterns typically form in a RD system when a fast diffusing inhibitor and a slow diffusing activator species are both present [20]. The stationary patterns we observe here are non-equilibrium structures (or dissipative structures) because they only exist under reaction conditions. Whether the original definition of Turing applies is not clear because, firstly, it has not been shown that they bifurcate from a spatially homogeneous state. Secondly, the domain boundaries are of obvious importance for the development of these patterns whereas a Turing pattern should possess an intrinsic wavelength. We therefore denote them as Turing-like structures.

From the information gathered so far we can identify some of the key mechanistic elements for the formation of the Turing-like patterns. Oxygen is more strongly bound to Rh than to Pt and therefore adsorbed oxygen “pulls” out the Rh from a Pt film that is alloyed with some Rh [21–25]. The enrichment of Rh in turn enhances the adsorption rate of oxygen because the oxygen sticking coefficient is higher on Rh than on Pt surfaces [26,27]. Thus a positive feedback exists between oxygen adsorption and Rh enrichment. This means that we have a process with autocatalytic kinetics and in terms of an activator/inhibitor model we thus have some kind of activator in our system. On the other hand, atomic hydrogen diffuses very rapidly and since it reactively removes oxygen, its role with respect to Rh enrichment is antagonistic to that of oxygen. At present, however, it would be premature to suggest a mechanistic scheme for the formation of the Turing-like patterns because it is not clear whether the bright spots are due to subsurface oxygen or an OH species and the role of potassium still needs to be identified. Subsequent experiments in which potassium was deliberately added to composite Rh(110)/Pt catalysts indicate that the potassium is in fact an essential constituent of the patterns discussed here.

With respect to the mechanism we can state the following. Firstly, we have identified an autocatalytic process which is coupled to the segregation of one of the metallic components. Secondly, it is evident that species with vastly different diffusion constants are present in our system and that these species are coupled to the autocatalytic process. The presence of species with strongly different diffusion constituents was shown to be one of the key requirements for the formation of Turing structures [17,20].

In summary, we have demonstrated that diffusion instabilities in catalytic surface reactions may give rise to a spatially modulated composition of alloyed surfaces. In these Turing-like patterns the catalyst itself is a dissipative structure changing its composition in response to varying parameters. The results presented here thus demonstrate very clearly the importance of dynamic effects in heterogeneous catalysis. They show that a purely static analysis in terms of a fixed surface composition and surface structure does not suffice to understand the functioning of real catalysts.

Acknowledgement

We thank Diego Lonza for his excellent technical assistance. We acknowledge Dr. M. Gentili and his group from IESS for developing and providing the zone plate optics. This work was financially supported by the BMBF (FRG), EC grant under Contract No. EBRCH-GECT920013 and Sincrotrone Trieste SCpA.

References

[1] M. Flytzani-Stephanopoulos and L.D. Schmidt, Prog. Surf. Sci. 9 (1979) 83.
[2] G.A. Somorjai and M.A. van Hove, Prog. Surf. Sci. 30 (1989) 201.
[3] R. Imbihl and G. Ertl, Chem. Rev. 95 (1995) 697.
[4] M.D. Graham, I.G. Kevrekidis, K. Asakura, J. Lauterbach, K. Krischer, H.H. Rotermund and G. Ertl, Science 264 (1994) 80;
M.D. Graham, M. Bär, I.G. Kevrekidis, K. Asakura, J. Lauterbach, H.H. Rotermund and G. Ertl, Phys. Rev. E 52 (1995) 76.
[5] E. Schütz, N. Hartmann, I.G. Kevrekidis and R. Imbihl, Catal. Lett. 54 (1998) 181.
[6] F. Mertens and R. Imbihl, Chem. Phys. Lett. 242 (1995) 221.
[7] M. Fassihi, V.P. Zhdanov, M. Rinnemo, K.-E. Keck and B. Kasemo, J. Catal. 141 (1993) 438.
[8] W. Engel, M.E. Kordesch, H.H. Rotermund, S. Kubala and A. von Oertzen, Ultramicroscopy 36 (1991) 148.
[9] M. Marsi, L. Casalis, L. Gregoratti, S. Günther, A. Kolmakov, J. Kovac, D. Lonza and M. Kiskinova, J. Electron Spectrosc. Relat. Phenom. 84 (1997) 73.
[10] J. Lauterbach, K. Asakura and H.H. Rotermund, Surf. Sci. 313 (1994) 52;
H.H. Rotermund, J. Lauterbach and G. Haas, Appl. Phys. A 57 (1993) 507.
[11] N.M.H. Janssen, A. Schaak, B.E. Nieuwenhuys and R. Imbihl, Surf. Sci. 364 (1996) L555.
[12] F. Mertens and R. Imbihl, Nature 370 (1994) 124.
[13] E.G. Seebauer, A.C.F. Kong and L.D. Schmidt, J. Chem. Phys. 88 (1988) 6597;
G. Hoogers, B. Lesiak-Orlowska and D.A. King, Surf. Sci. 327 (1995) 47.
[14] J.L. Gland, B. Sexton and G.B. Fisher, Surf. Sci. 95 (1980) 587.
[15] G. Broden, G. Pirug and H.P. Bonzel, Chem. Phys. Lett. 73 (1980) 506.

[16] A.M. Turing, Philos. Trans. Roy. Soc. London B 237 (1952) 37.
[17] J.D. Murray, *Mathematical Biology* (Springer, Berlin, 1990).
[18] J. Falta, R. Imbihl and M. Henzler, Phys. Rev. Lett. 64 (1990) 1409.
[19] V. Castets, E. Dulos, J. Boissonade and P. De Kepper, Phys. Rev. Lett. 64 (1990) 2953;
Q. Ouyang and H.L. Swinney, Nature 352 (1991) 610.
[20] A.S. Mikhailov, *Foundations of Synergetics I* (Springer, Berlin, 1994).
[21] Y. Matsumoto, Y. Okawa, T. Fujita and K. Tanaka, Surf. Sci. 355 (1996) 109.
[22] H. Tamura, A. Sasahara and K. Tanaka, Surf. Sci. 303 (1994) L379.
[23] F.C.M.J.M. van Delft, J. Siera and B.E. Nieuwenhuys, Surf. Sci. 208 (1989) 365.
[24] A. Sasahara, H. Tamura and K.I. Tanaka, J. Phys. Chem. 101 (1997) 1186.
[25] I. Toyoshima and G.A. Somorjai, Catal. Rev. Sci. Eng. 19 (1979) 105.
[26] G. Comelli, V.R. Dhanak, M. Kiskinova, K.C. Prince and R. Rosei, Surf. Sci. Rep. 32 (1998) 165.
[27] C.T. Campbell, G. Ertl, H. Kuipers and J. Segner, Surf. Sci. 107 (1981) 220;
Y.Y. Yeo, L. Vattuone and D.A. King, J. Chem. Phys. 106 (1997) 392.